

Design Considerations of a Packed Calcite Bed for Hardening Desalinated Water

Hilla Shemer, David Hasson,* and Raphael Semiat

Rabin Desalination Laboratory, Technion-Israel Institute of Technology, Haifa 32000, Israel

ABSTRACT: Desalinated water is poor in minerals, making it corrosive and unpalatable. A certain degree of remineralization is necessary in order to overcome these problems as well as to meet health requirements. A commonly used remineralization process is to pass desalinated water dosed with either CO₂ or H₂SO₄ through a bed of limestone, reintroducing bicarbonate alkalinity and calcium hardness to the water. The paper presents cumulative experimental evidence confirming the reliability of the kinetic model developed by Yamauchi et al. and Letterman et al. The paper also analyzes the main operational parameters affecting the minimum cost design of a hardening column. Finally, the viability of incorporating a CO₂ desorption process so as to reduce alkali consumption is examined.

1. INTRODUCTION

Since desalinated water is practically devoid of minerals, a certain degree of remineralization is necessary in order to meet health requirements and make the water palatable and noncorrosive. Nevertheless, water quality goals for post-treatment processes are most often site-specific based on the water source, the membrane process, and the existing water system. Duranceau et al.¹ conducted a survey of industry practice of post-treatment stabilization of desalinated water. On the basis of this information, guiding water quality specifications were proposed. The guidelines are listed in Table 1, along

Table 1. Water Quality for Remineralized Desalinated Water

parameter	seawater ¹	brackish water ¹	Israeli regulation ²
pH	6.5–9.5	7.5–8.4	7.5–8.3
alkalinity (mg/L as CaCO ₃)	50–125	75–150	>80
calcium (mg/L as CaCO ₃)	70–75	60–100	80–120
hardness (mg/L as CaCO ₃)	50–85	75–110	160–240
TDS (mg/L)	100–500	85–350	
turbidity (NTU)	0.6–3.0	0.2–2.0	<0.5
boron (mg/L)	0.5–1	not applicable	
bromide (mg/L)	<0.3	<0.3	
LSI			>0
CCPP			3–10

with the Israeli regulations.² The proposed guidelines are seen to differ from the Israeli regulations; Duranceau et al.¹ differentiate between sea and brackish water sources and include some requirements absent from the Israeli regulations.

Blending desalinated water with source water or partially treated water is a common post-treatment practice. Another approach is to reintroduce some essential ions to the desalinated water in order to achieve a balanced mineral content. A commonly used remineralization process is to contact CO₂ acidified desalinated water with a packed bed of limestone. Limestone dissolution provides two ingredients to the water bicarbonate alkalinity and calcium hardness:



Excess CO₂ is required in order to accomplish the limestone dissolution to the required calcium hardness in a reasonably sized column. The residual CO₂ acidity of the hardened water is neutralized by adding NaOH or Na₂CO₃ in order to reach the specified pH.³

As shown below, the CO₂ consumption represents a major cost item of limestone remineralization. A possible option is to recover the residual CO₂ by air stripping or using a vacuum pump or an eductor. Eductor suction of CO₂ was claimed to have potential advantages over a vacuum pump, and they include lower operation cost, simplicity, reliability, ease of installation, nonelectrical requirement, and corrosion and erosion resistance. However, these advantages were not realized in a pilot plant trial.⁴

Results of several studies indicate that limestone dissolution is affected by the crystal habit of the specific calcite pellets, their inner porosity, and their impurities content (inorganic ions such as PO₄, Pb, Cd, Cu, Zn, Fe, and Mn and organic matter).^{5–7} The fundamental dissolution mechanism is still not sufficiently clear. One theory claims that the actual dissolution occurs on edges of the mineral surface. Far from equilibrium, new edges can be easily created, but close to equilibrium the chemical driving force is too limited to create new edges. These active pits can be closed by inhibitors causing reaction rates to drop dramatically.⁸

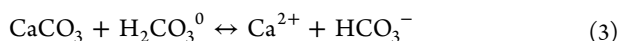
Several theoretical and practical models used to describe the dissolution of calcite are available. The theoretical model developed by Plummer et al.⁹ neglects mass transfer considerations and assumes that the dissolution is governed by the following three simultaneous reactions:

Special Issue: Enrico Drioli Festschrift

Received: October 30, 2012

Revised: February 21, 2013

Accepted: February 25, 2013



Several researchers proposed modifications to the Plummer et al. model so as to adapt it to limestone contactors.¹⁰ Ultimately, it appears that the only reliable models for design of packed bed limestone contactors are described in publications authored by Yamauchi et al.,¹¹ Letterman et al.,^{12,13} Hasson and Bendrihem,³ and Shemer et al.¹⁴ The model proposed by Yamauchi et al. for the CO₂ hardening process assumes that calcite dissolution is mass-transfer controlled. The driving force is then the difference between the bulk CO₂ concentration and the equilibrium CO₂ concentration ([CO₂]_e). The resulting depletion of the dissolved CO₂ in the water percolating through the limestone column is given by:

$$\ln \frac{[\text{CO}_2]_L - [\text{CO}_2]_e}{[\text{CO}_2]_0 - [\text{CO}_2]_e} = -k \frac{6(1-\varepsilon)L}{d_p \Phi u} \quad (5)$$

where [CO₂]₀, [CO₂]_L, and [CO₂]_e are the inlet, bed height *L*, and equilibrium concentrations of the carbon dioxide, respectively; *k* is the reaction rate coefficient; ε is the fractional bed porosity; *L* is the bed length (mm); *d_p* is the particle diameter (mm); Φ is the shape factor (sphericity); and *u* is the superficial flow velocity (mm/s).

Material balance relations show that eq 5 also holds for concentration changes of the calcium and bicarbonate ions:²

$$\begin{aligned} \ln \frac{[\text{HCO}_3]_e - [\text{HCO}_3]_L}{[\text{HCO}_3]_e - [\text{HCO}_3]_0} \\ = \ln \frac{[\text{Ca}]_e - [\text{Ca}]_L}{[\text{Ca}]_e - [\text{Ca}]_0} \\ = -k \frac{6(1-\varepsilon)L}{d_p \Phi u} \end{aligned} \quad (6)$$

The equilibrium concentrations are given by:³

$$\begin{aligned} [\text{CO}_2]_e &= \frac{K_2}{2K_1K_{sp}} \times [\text{HCO}_3^-]_e^3 \\ &= [\text{CO}_2]_0 - \frac{1}{2}[\text{HCO}_3^-]_e \\ &= [\text{CO}_2]_0 - [\text{Ca}]_e \end{aligned} \quad (7)$$

where *K*₁ and *K*₂ are the first and second dissociation constants of carbonic acid, respectively, and *K*_{sp} is the solubility product of CaCO₃.

Yamauchi et al.¹¹ showed a very good fit of pilot plant data to the above model. This was also observed by extensive data obtained by Hasson and Bendrihem³ and Shemer et al.,¹⁴ part of which are presented below. Shemer et al.¹⁴ obtained the following temperature correlation for limestone pellets denoted in this paper as limestone-A of average size of 2 mm:

$$\frac{6k}{\Phi} (\text{mm/s}) = (1.06 \times 10^7) \times \exp \left(-\frac{52000}{RT} \right) \quad (8)$$

Letterman et al.¹² developed a design model based on mineral acid dissolution of calcite. His kinetic equation is based on the calcium driving force of eq 6, but with a modification correcting for the deviation from plug flow using a dispersion

model. The magnitude of dispersion correction is minor. The Letterman et al. design equation is virtually identical to the Yamauchi et al. equation. Interestingly, these two studies were conducted independently at the same period of time.

Letterman and Kothari^{15,16} developed a computer program (DESCON) based on the Letterman et al.¹² model. This computer program can be used to determine the required depth of limestone bed given the influent water chemistry, superficial velocity the physical and chemical characteristics of the limestone and the treatment objectives. Another computer program based on the Letterman et al. model was developed by Schott¹⁷ ("Limestone Bed Contactor: Corrosion Control and Treatment Process Analysis Program"). This program calculates the depth of the limestone bed, empty bed contact time, and limestone dissolved per volume of water treated from the initial to equilibrium condition. Other additional parameters that are calculated using this program include pH, total alkalinity, CO₂ concentration, dissolved inorganic carbon, and calcium content.

The present paper consolidates the reliability of the Yamauchi et al. model by examining CO₂ dissolution of limestone pellets of two different sources and that of Letterman et al. by analyzing recent published data on H₂SO₄ limestone dissolution. Design of a limestone column, taking into account the capital, energy, and chemical costs, is discussed. The viability of incorporating a CO₂ desorption process so as to reduce alkali consumption is also analyzed.

2. EXPERIMENTAL SECTION

Dissolution experiments were conducted using two Perspex columns (1.8 m height × 98 mm ID) connected in series. Each column was filled to a height of 94 cm with limestone pellets. A schematic description of the experimental setup is presented elsewhere.¹⁴ Calcite pellets obtained from two different sources were used (Table 2). The average particle size of each of the two tested pellets was specified by the manufacturers to be 2 mm.

Table 2. Properties of the Limestone Pellets

	pellets A	pellets B
size range (mm)	1.5–2.5	1.0–3.0
purity	>96% CaCO ₃	>97.5% CaCO ₃
porosity (ε)	56%	51%
supplier	Zmitut 81 (Israel)	Negev Industrial Minerals (Israel)

The limestone dissolution path along the packed bed was followed by monitoring the composition of water extracted from 15 sampling points located along the length of the two columns. Each sample was analyzed to determine its pH, alkalinity, and calcium concentration. The dissolution kinetic coefficients were measured at a superficial flow velocity of 4.56 mm/s, at three CO₂ concentrations (3.0, 4.5, 6.4 mmol/L) and at the average water temperature of 28.6 °C.

Figure 1 shows a schematic diagram of the CO₂ air stripping system consisting of a glass column (50 cm height × 50 mm ID) filled with 1/2 in. Raschig rings. Water containing CO₂ was fed to the top of the column, and air was introduced at the bottom to provide countercurrent flow. Experiments were conducted at a constant water flow rate of 2.1 L/min, at air flow rates ranging between 2.7 and 42.1 L/min at atmospheric pressure and at CO₂ concentrations of 0.7–2.5 mmol/L.

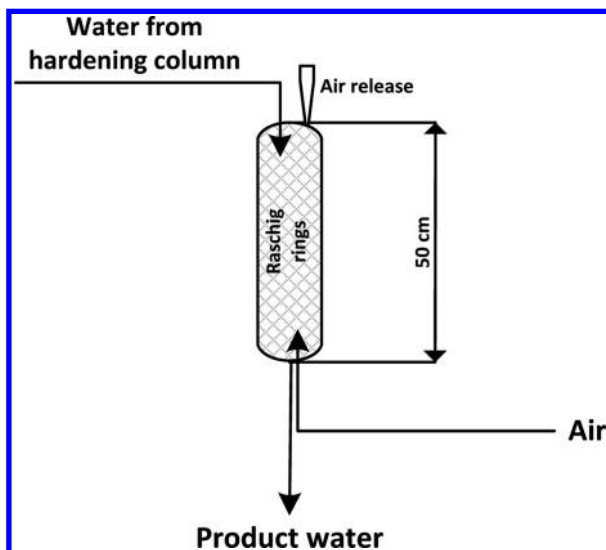


Figure 1. Schematic diagram of the air stripping setup.

3. RESULTS

3.1. Remineralization Kinetics. The Yamauchi et al.¹¹ model (eq 6) predicts a linear relationship for the plot of $\ln\left(\frac{[Ca^{2+}]_e - [Ca^{2+}]_L}{[Ca^{2+}]_e - [Ca^{2+}]_0}\right)$ or $\ln\left(\frac{[HCO_3^-]_e - [HCO_3^-]_L}{[HCO_3^-]_e - [HCO_3^-]_0}\right)$ versus the bed height L . The subscripts e, L, and 0 stand for inlet, bed height, and equilibrium concentrations, respectively. The slope of the line yields the value of the kinetic coefficient $6k/\Phi$. The experimental data conformed very well to the Yamauchi et al. model, as illustrated in Figure 2. The profiles of both the

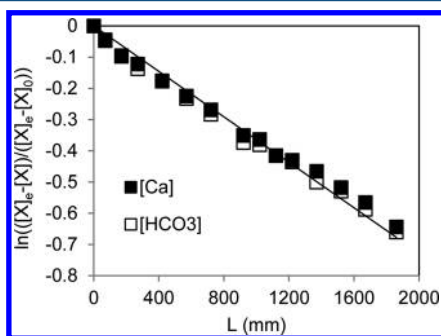


Figure 2. Plot of $\ln\left(\frac{[X]_e - [X]_L}{[X]_e - [X]_0}\right)$ versus the bed height L (X represents either $[HCO_3^-]$ or $[Ca^{2+}]$).

bicarbonate and calcium ions given by eq 6 are seen to fall on identical straight lines passing through the origin with a correlation coefficient $R^2 > 0.99$.

The runs performed with limestone A gave the average value of $6k/\Phi = (1.05 \pm 0.16) \times 10^{-2}$ mm/s, whereas a higher average value of $(1.76 \pm 0.06) \times 10^{-2}$ mm/s was obtained with limestone B. The excellent fit of the experimental dissolution profile to the Yamauchi et al. model is further illustrated in Figure 3 which compares the experimental alkalinity data with the calculated values, for limestone A, along the dissolution paths. The predicted values were calculated using the following parameters: $(1 - \epsilon) = 0.44$; $d_p = 2$ mm; $6k/\Phi = 1.05 \times 10^{-2}$ mm/s.

Remarks in papers questioning the reliability of the Yamauchi and Letterman models are unjustified.^{18,19} In particular it seems rather odd that the more recent paper¹⁹ which carried out

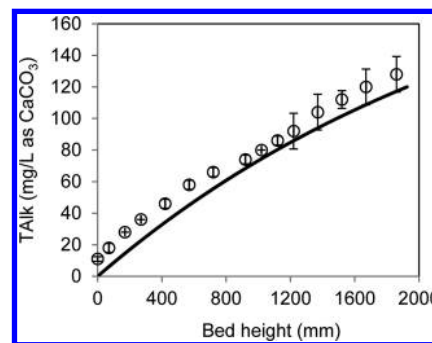


Figure 3. Comparison of measured alkalinity (circles) with predicted values (line) for limestone A dissolution at $[CO_2]_0 = 3.0$ mmol/L.

experimental measurements of H_2SO_4 -based calcite dissolution failed to test the data against the well-established models.

The experimental data of the above publication were analyzed on the basis of the available of Yamauchi and Letterman theory. Equation 6 was used to predict the experimental results measured at the following conditions: bed height of 426 cm, average pellet diameter of 0.3 cm, bed porosity of 0.53, and H_2SO_4 concentrations of 5.0 and 7.4 mmol/L. Values of $[Ca]_e$ were calculated using Minteq Version 3.0. The mass transfer coefficients k , obtained by analyzing the data of the six runs 1a through 3b,¹⁹ were found to fit very well the following correlation:

$$\frac{6k}{\Phi} \text{ (cm/s)} = 2.7 \times 10^{-3} \sqrt{u \text{ (cm/s)}} \quad (9)$$

This result conforms to the Wilson and Geankoplis²⁰ correlation described below but with k values 1/3 smaller. Figure 4 shows that the dissolution data measured by Lehmann et al.¹⁹ perfectly fit the Letterman model.

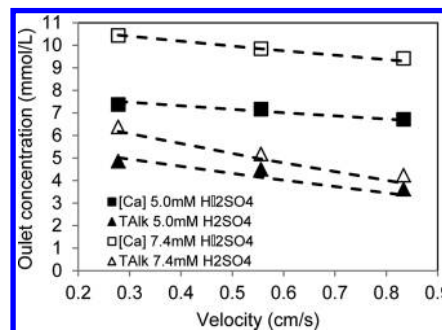


Figure 4. Comparison of experimental calcium and total alkalinity measurements (symbols) with predicted values (dashed lines).

To conclude, cumulative experimental evidence on limestone dissolution confirms the reliability of the kinetic model developed by Yamauchi et al. and Letterman et al.

3.2. Surface Reaction Effect. The basic design equations assume mass transfer control. In principle it should be possible to predict the dissolution coefficient from mass transfer correlations in flow through packed beds. There are numerous mass transfer correlations in the literature which show variations among them. Calculations from a few published correlations gave dissolution coefficient values of the right order of magnitude but with some deviations from the coefficients observed in this study. For example, the correlation of Wilson

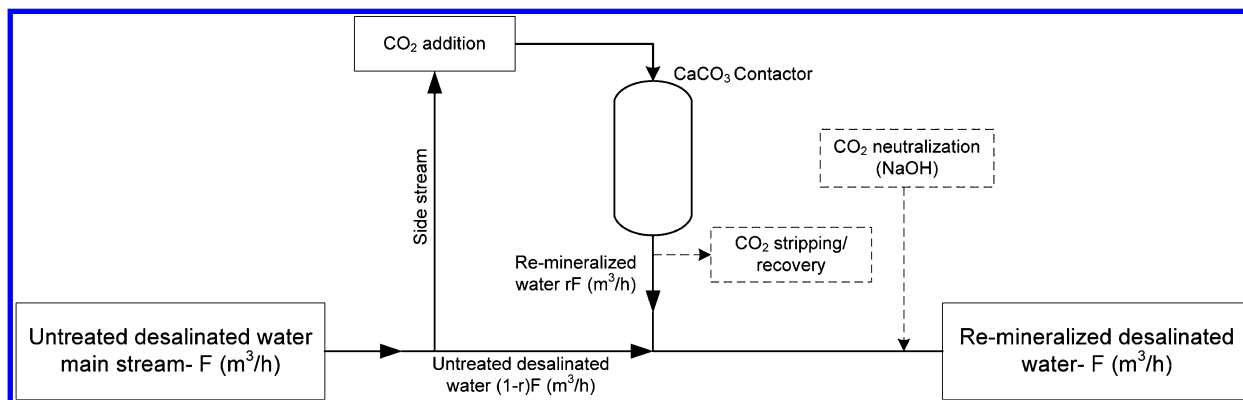


Figure 5. Schematic flow sheet of a split remineralization system (r represents fractional flow of the treated water).

and Geankoplis²⁰ has the following form in the range of $0.0016 < Re < 55$ and $0.35 < \epsilon < 0.75$:

$$J_D = \frac{k}{u} \left(\frac{\mu/\rho}{Dv} \right)^{2/3} = 1.09(Re')^{-2/3} \quad (10)$$

where $Re' = d_p u \rho / \mu$. Dv is the ion diffusivity, μ is the water viscosity, and ρ is the water density. The predicted mass transfer coefficient for the experimental conditions using the CO_2 diffusivity value of $2 \times 10^{-5} \text{ cm}^2/\text{s}$ is $1.36 \times 10^{-2} \text{ mm/s}$, compared with the experimental values of 1.05×10^{-2} and $1.76 \times 10^{-2} \text{ mm/s}$ for limestone A and limestone B, respectively.

The correlation used by Letterman et al.¹² is

$$J_D = \frac{k}{u} \left(\frac{\mu/\rho}{Dv} \right)^{2/3} = 5.7(Re)^{-0.78} \quad 1 < Re < 30 \quad (11)$$

where $Re = d_p u \rho / \mu(1 - \epsilon)$. This correlation predicts a higher mass transfer coefficient of $3.69 \times 10^{-2} \text{ mm/s}$.

Two conclusions can be drawn from the above analysis. It is clear that there is a need for developing a reliable mass transfer coefficient correlation for flow through packed bed of calcite hardening pellets. The more important observation is that two calcite pellets of different character give significantly different values for the kinetic coefficient under identical hydrodynamic flow conditions. This reaffirms the findings of Letterman²¹ and Ruggieri et al.²² that the dissolution of calcite is influenced not only by mass transfer considerations but also by some surface reaction effects.

3.3. Economic Considerations. Operation of limestone contactors may be limited by the large dimension columns required for high capacity desalination plants. Reduction of column size is possible by hardening to a high level only part of the desalinated water and blending it with the main stream so as to meet water quality requirements (Figure 5).

The main operational parameters affecting the minimum cost design of a hardening column based on specific limestone pellets are the packed column height, the inlet CO_2 concentration, and the blending ratio of remineralized water with nontreated desalinated water. As evident from the kinetics of dissolution (eqs 5 and 6), a high inlet CO_2 concentration enables attainment of the desired calcium concentration in a shorter column. However, to meet the required alkalinity and pH conditions, the residual CO_2 needs to be neutralized with NaOH or recovered, as indicated by dashed lines in Figure 5. When remineralizing only a fraction of the desalinated water and then blending it with the untreated water, higher hardening

levels are required calling for higher inlet CO_2 concentrations. The optimal design is obtained when the total cost, composed of the amortized cost of the hardening column and the cost of the chemicals CO_2 and NaOH, is at a minimum.

Figure 6 illustrates the principle of the optimization method for certain design conditions meeting Israeli product water

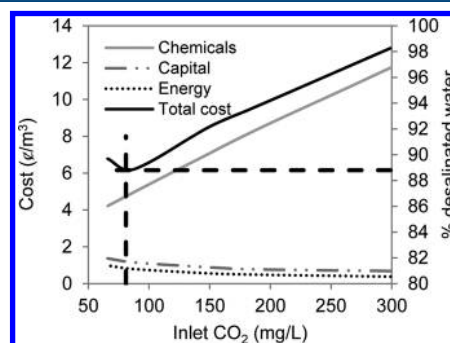


Figure 6. Economic optimization of a desalinated water remineralization process.

quality regulations. This figure describes three cost components: energy, capital, and chemicals (CO_2 and NaOH). It is evident that chemicals are the major contributor to the total cost. The minimal cost for the above example presented in Figure 6 is at inlet CO_2 of 81 mg/L and a remineralization of 89% of the desalinated water.

3.4. CO_2 Desorption. As shown in the above economic analysis, chemicals represent the major cost item. Desorption of excess CO_2 by air stripping was studied as an alternative to its neutralization using NaOH. This technique can be further used to recover and reuse the stripped CO_2 . Figure 7 presents CO_2 removal as a function of the ratio of water (Q_L) to air (Q_G) flow rates for $Q_L = 2.1 \text{ L/min}$ and a bed height Z of 0.5 m.

Using the literature value of $HTU_{OL} = 0.4 \text{ m}$,²³ the data of Figure 7 were found to fit closely the theoretical predictions calculated by the following equations:

$$Z = HTU_{OL} \cdot NTU_{OL} \quad (12)$$

where HTU_{OL} is the height of a transfer and NTU_{OL} is the number of transfer units defined by:

$$NTU_{OL} = \frac{\ln \left\{ (1 - A) \left(\frac{x_2 - \frac{y_1}{m}}{x_1 - \frac{y_1}{m}} \right) + A \right\}}{1 - A} \quad (13)$$

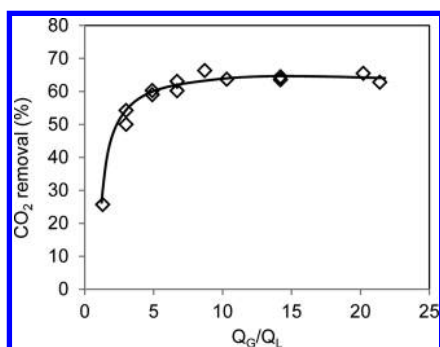


Figure 7. Experimental and predicted CO₂ removal as a function of the water to air flow rates ratio.

Here, x_1 is mole fraction of CO₂ in water effluent, x_2 is the mole fraction of CO₂ in water influent, y_1 is the mole fraction of CO₂ in air influent, m is equilibrium solubility of CO₂, and $A = L/G \times m$; L and G are molar liquid and gas flow per unit of stripper cross sectional area, respectively (kg mol/(m² s)).

In conclusion, the close agreement between the experimental results with the predicted values indicates that conventional stripping theory can be readily applied for economic evaluation of the CO₂ stripping process for a specific hardening column design.

4. CONCLUSIONS

The experimental results of this study reaffirm the validity of the Yamauchi et al. and Letterman et al. model for designing a remineralization hardening column operated by CO₂ or H₂SO₄ dissolution of calcite pellets. It is shown that the main parameters governing the minimum cost design of a hardening column are the limestone pellets size and mineralogy, the inlet CO₂ concentration, the residual CO₂ neutralization, and the blending ratio of remineralized water with nontreated desalinated water.

AUTHOR INFORMATION

Corresponding Author

*Tel.: +972-4-8292936. Fax: +972-4-8295672. E-mail: Hasson@tx.technion.ac.il.

Notes

The authors declare no competing financial interest.

REFERENCES

- (1) Duranceau, S. J.; Wilder, R. J.; Douglas, S. S. Guidance and recommendations for posttreatment of desalinated water. *J. Am Water Works Assoc.* **2012**, *104*, 510–520.
- (2) Israeli Ministry of Health. Drinking water quality standards, Jan. 2012; p 33 (Hebrew text).
- (3) Hasson, D.; Bendrihem, O. Modeling remineralization of desalinated water by limestone dissolution. *Desalination* **2006**, *190*, 189–200.
- (4) De Souza, P. F.; Du Plessis, G. J.; Mackintosh, G. S. An evaluation of the suitability of the limestone based sidestream stabilization process for stabilization of waters of the Lesotho Highlands Scheme. Presented at the Biennial Conference of the Water Institute of Southern Africa, Durban, South Africa, May 19–23, 2002.
- (5) Terjesen, S. G.; Erga, O.; Thorsen, G.; Ve, A. The inhibitory action of metal ions on the formation of calcium bicarbonate by the reaction of calcite and aqueous carbon dioxide. *Chem. Eng. Sci.* **1961**, *14*, 277–289.
- (6) Gutjahr, A.; Dabringhaus, H.; Lacmann, R. Studies of the growth and dissolution kinetics of the CaCO₃ polymorphs calcite and

aragonite. II. The influence of divalent cation additives on the growth and dissolution rates. *J. Cryst. Growth* **1996**, *158*, 310–315.

(7) Van Tonder, G. J.; Schutte, C. F. The effect of metal cations on the kinetics of limestone neutralisation of acid waters. *Environ. Technol.* **1997**, *18*, 1019–1028.

(8) Gude, J. C. J.; Schoonenberg Kegel, F.; van de Ven, W. J. C.; de Moel, P. J.; Verberk, J. Q.; van Dijk, J. C. Micronized CaCO₃: a feasible alternative to limestone filtration for conditioning and (re)-mineralization of drinking water. *J. Water Supply: Res. Technol.* **2011**, *60*, 469–477.

(9) Plummer, L. N.; Wigley, T. M. L.; Pakhurst, D. L. The kinetics of calcite dissolution in CO₂-water system at 5°C to 60°C and 0.0 to 1.0 atm. CO₂. *Am. J. Sci.* **1978**, *278*, 179–216.

(10) Bang, D. P. Upflow limestone contactor for soft and desalinated water. M.S. Thesis, Delft University of Technology, Delft, August 2012.

(11) Yamauchi, Y.; Tanaka, K.; Hattori, K.; Kondo, M.; Ukawa, N. Remineralization of desalinated water by limestone dissolution. *Desalination* **1987**, *60*, 365–383.

(12) Letterman, R. D.; Driscoll, C. T.; Haddad, M.; Hsu, H. A. Project summary: limestone bed contactors for control of corrosion at small water utilities. EPA document EPA/SR809979-01-3; U.S. Environmental Protection Agency: 1987.

(13) Letterman, R. D. Kothari, S. *Design tools for limestone contactors*; EPA document, Cooperative Agreement CR814926, U.S. Environmental Protection Agency: 1993.

(14) Shemer, H.; Hasson, D.; Semiat, R.; Priel, M.; Nadav, N.; Shulman, A.; Gelman, E. Remineralization of desalinated water by limestone dissolution with carbon dioxide. *Desalin. Water Treat.* **2013**, *51*, 877–881.

(15) Letterman, R. D.; Hadad, M.; Driscoll, C. T. Limestone contactors-steady-state design relationships. *J. Environ. Eng.* **1991**, *117*, 339–358.

(16) Letterman, R. D.; Kothari, S. *Instruction for using Descon: A computer program for the design of limestone contactor*; CR 814926; U.S. Environmental Protection Agency: 1995.

(17) Schott, G. *Limestone bed contactor - Corrosion control and treatment process analysis program*, Version 1.02; 2003.

(18) Birnhack, L.; Voutchkov, N.; Lahav, O. Fundamental chemistry and engineering aspects of post-treatment processes for desalinated water - a review. *Desalination* **2011**, *273*, 6–22.

(19) Lehmann, O.; Birnhack, L.; Lahav, O. Design aspects of calcite-dissolution reactors applied for post treatment of desalinated water. *Desalination* **2013**, *314*, 1–9.

(20) Wilson, E. J.; Geankoplis, C. J. Liquid mass transfer at very low Reynolds numbers in packed beds. *Ind. Eng. Chem. Fundam.* **1966**, *5*, 9–14.

(21) Letterman, R. D. *Project summary: calcium carbonate dissolution rate in limestone contactors*; EPA document EPA/600/SR-95/068; U.S. Environmental Protection Agency: 1995.

(22) Ruggieria, F.; Fernandez-Turiela, J. L.; Gimeno, D.; Valeroc, F.; Garcias, J. C.; Medinac, M. E. Limestone selection criteria for EDR water remineralization. *Desalination* **2008**, *227*, 314–326.

(23) Sherwood, T. K.; Pigford, R. L. *Absorption and Extraction*; McGraw-Hill: New York, 1952.